

NANO EXPRESS

Open Access

Photoluminescence characteristics of $\text{Cd}_{1-x}\text{Mn}_x\text{Te}$ single crystals grown by the vertical Bridgman method

Younghun Hwang¹, Youngho Um^{2*} and Hyoyeol Park³

Abstract

In this paper, we report a systematic investigation of band-edge photoluminescence for $\text{Cd}_{1-x}\text{Mn}_x\text{Te}$ crystals grown by the vertical Bridgman method. The near-band-edge emissions of neutral acceptor-bound excitons (labeled as L1) were systematically investigated as a function of temperature and of alloy composition. The parameters that describe the temperature variation of the energy were evaluated by the semiempirical Varshni relation. From the temperature dependence of the full width at half maximum of the L1 emission line, the broadening factors $\Gamma(T)$ were determined from the fit to the data. The activation energies of thermal quenching were obtained for the L1 peak from the temperature dependence of the bound exciton peaks and were found to decrease with increasing Mn concentration.

Keywords: $\text{Cd}_{1-x}\text{Mn}_x\text{Te}$, Bridgman method, PL, exciton, broadening, thermal quenching

Introduction

Diluted magnetic semiconductors [DMSs] are semiconductor alloys formed by randomly replacing a fraction of the cations in a compound semiconductor with magnetic ions, e.g., Mn^{2+} in CdTe to form $\text{Cd}_{1-x}\text{Mn}_x\text{Te}$ [1]. The presence of the magnetic ions leads to a number of unusual electronic, optical, and magneto-optical properties, including the ability to magnetically tune the band gap made possible in this material by the large $sp-d$ exchange interaction between magnetic ions and band electrons [2]. These properties make $\text{Cd}_{1-x}\text{Mn}_x\text{Te}$ [CMT] promising candidates for fabricating magneto-optical devices, such as Faraday rotators, isolators, magneto-optical switches, and solar cells [3]. Recently, CMT has attracted much interest as a potential material for applications in the gamma-ray detectors because of a wide band gap and high resistivity [4]. The bulk CMT crystals have been grown with different growth methods, such as vertical gradient freeze, traveling heater, and vertical Bridgman method. Among these, the vertical Bridgman technique can be widely used successfully to grow CMT bulk crystals. The CMT crystals fabricated by this method showed zinc-blende structures

for $x < 0.77$ [1]. Photoluminescence [PL] is a useful technique that has been employed to characterize bulk materials [5]. This technique has been used to study the near-band-edge excitonic states and structural quality in materials. In particular, the temperature dependence of PL spectrum intensity has been used to obtain information about electronic gap levels in semiconductors.

In this work, we present the PL study on the CMT bulk crystals grown by the vertical Bridgman method to investigate the variation of the band-edge transition energy in the PL spectra as a function of Mn composition x and temperature. In addition, the measurements made it possible to analyze and discuss in detail the broadening mechanisms of the exciton emission lines and their dependence on both the Mn content and temperature.

Experiment

CMT crystals were grown by using the vertical Bridgman method from $\text{Cd}(6\text{N})$, $\text{Te}(6\text{N})$, and $\text{Mn}(4\text{N})$ elements. The elements were vacuum-sealed in a carbon-coated quartz ampule under a pressure of 1×10^{-6} Torr. The reaction temperature was slowly raised from 600°C to $1,200^\circ\text{C}$. The ampule was held at $1,200^\circ\text{C}$ for 3 h to homogenize the melt and lowered at a rate of 1.44 mm/h. The solidification gradient in the furnace was $22.5^\circ\text{C}/\text{cm}$. The crystal

* Correspondence: yhum@ulsan.ac.kr

²Department of Physics, University of Ulsan, Ulsan, 680-749, South Korea
Full list of author information is available at the end of the article

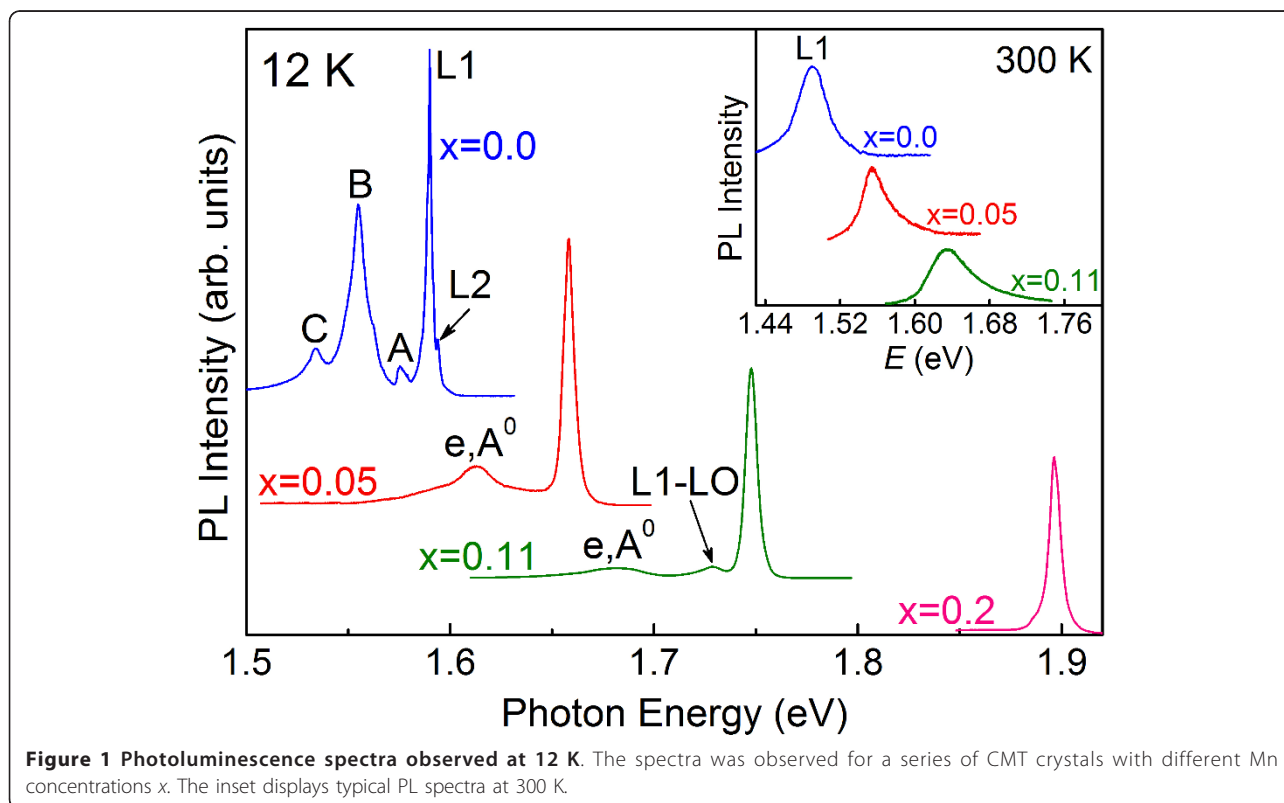
obtained was of cylindrical form of 10 mm in diameter and 20 mm long. The mole fraction x was determined by an electron probe microanalyzer (EPMA-1400; Shimadzu Corporation, Nakagyo-ku, Kyoto, Japan). Before PL measurements, CMT samples were cut into $5 \times 5 \times 1 \text{ mm}^3$, mechanically polished, and then etched in 2% bromine-methanol solution. In order to measure the PL spectra, the samples were cooled down to 12 K in a cryogenic system and excited by a 442-nm line of a He-Cd laser (Liconix 4240NB; Sunnyvale, CA, USA). The luminescence was detected by a photomultiplier tube using a grating monochromator and analyzed by a computer-aided data acquisition system.

Results and discussion

Figure 1 shows the PL spectra at 12 K and 300 K taken on the CMT crystals for Mn concentration from $x = 0.0$ to 0.2. In DMSs, the strong $sp-d$ exchange interaction between carriers and localized magnetic ions gives rise to the formation of a magnetic polaron and causes an energy shift as a result. However, we only considered the behavior of the exciton peak with temperature and composition without taking the formation of a magnetic polaron into account because our temperature was slightly high to show the bound magnetic polaron in the PL spectra, and there was no applied magnetic field. The PL spectra are dominated by exciton peaks, i.e., there is

no noticeable luminescence associated with self-activated or other deep centers. The band-edge emission peaks of a CdTe crystal are similar to those found in the PL spectra reported by other investigators [6,7], and it will therefore be convenient to use our results for CdTe as a point of departure.

The inset of Figure 1 shows the PL spectra for CMT with different Mn mole fractions at 300 K. The line shapes of the spectra taken at 300 K consist of a single band which corresponds to transitions across the band gap. The intense PL emission at 300 K in CdTe reflects that the samples are high quality crystals. The dominant emission peak observed for CdTe at 1.590 eV is attributed to neutral acceptor-bound exciton transitions (labeled L1). This acceptor bound exciton feature dominates in the PL spectrum observed from a range of grown CdTe samples which are usually p -type [8]. We ascribe the weaker higher-energy feature at 1.594 eV associated with bound exciton recombination about shallow donors (labeled L2) [9]. The spectra also show a weak luminescence peak at about 1.575 eV, which is identified as the first longitudinal-optical [LO]-phonon replica (designated as A) of the free exciton transition [7]. The spectra also show weak luminescence peaks at about 1.555 and 1.534 eV, which we interpreted to be the second and third LO-phonon replicas (designated as B and C) of the free exciton [7]. The general features of



the CdTe PL spectra are also seen for the CMT crystals. However, for $x > 0$, the L1 and L2 luminescence lines begin to overlap and can no longer be resolved because of the increase of line broadening which accompanies the increase of x . The main emission peaks at the highest energy are believed to be due to the acceptor bound exciton (L1). The weak peak at slightly lower energies, 1.612 and 1.681 eV for $x = 0.05$ and 0.11 in Figure 1 has been attributed to the electron-to-neutral acceptor transitions (e, A^0). The energy separation between L1 and (e, A^0) increases from 46 to 66 meV upon increasing x from 0.05 to 0.11, which is larger than the separation of 41 meV for CdTe [10]. In addition, the peak at 1.728 eV for $x = 0.11$ is the LO-phonon replica of the L1 transition giving a LO phonon energy of 21 meV in agreement with the published value of 21.4 meV [11]. The L1 peaks (as well as L2 when they are resolved) are blue shifted with increasing Mn mole fraction x . According to Lautenschlager et al. [12], this blueshift is responsible to the decrease of lattice constant, which is not strongly affected by the admixture of Mn $3d$ states. As the incorporation of Mn atoms increases, the band-edge luminescence peak becomes broader and weaker.

Figure 2 shows the temperature dependences of the L1 peak positions for a series of alloys with different Mn concentrations. The observed band-edge luminescence energy shows a clear blueshift with decreasing T . The solid curves in the figures were drawn by fitting to the L1 emission peak positions the empirical equation [13]

$$E_0(T) = E_0(0) - \alpha T^2 / (\beta + T), \quad (1)$$

where $E_0(0)$ is the transition energy at $T = 0$ K, and α and β are constants referred to as Varshni thermal coefficients. The parameter values of α and β obtained by fits to our $E_0(T)$ data with Equation 1 are listed in Table 1. The parameter α is seen to increase linearly with x . The change of the band-gap energy E_g with temperature is usually attributed to the effect of electrons or phonons. The electron-hole pair is believed to soften the lattice vibration of the crystal when it is excited across a band gap [14]. This change in lattice vibration frequency can also occur when carriers are bound to vacancies or when impurities are excited. The increase in the temperature parameter α with increasing x in CMT indicates that the crystal is undergoing changes in the lattice vibration frequency as the Mn content increases in the alloy lattice. One can argue that the introduction of Mn into the CdTe lattice leads to the formation of vacancy (acceptor, donor) sites on which electrons or holes can be trapped. The presence of a trapped carrier reduces the interatomic force constant at or around the vacancy site, thus softening the normal-mode frequencies of the lattice and reducing the zero-point energy of the oscillators. An increase in the number of Mn atoms in the lattice seems to lead to an increase in the effective mass of the bound trap complex, and thus to an increase in mode softening [15]. This fact agrees with

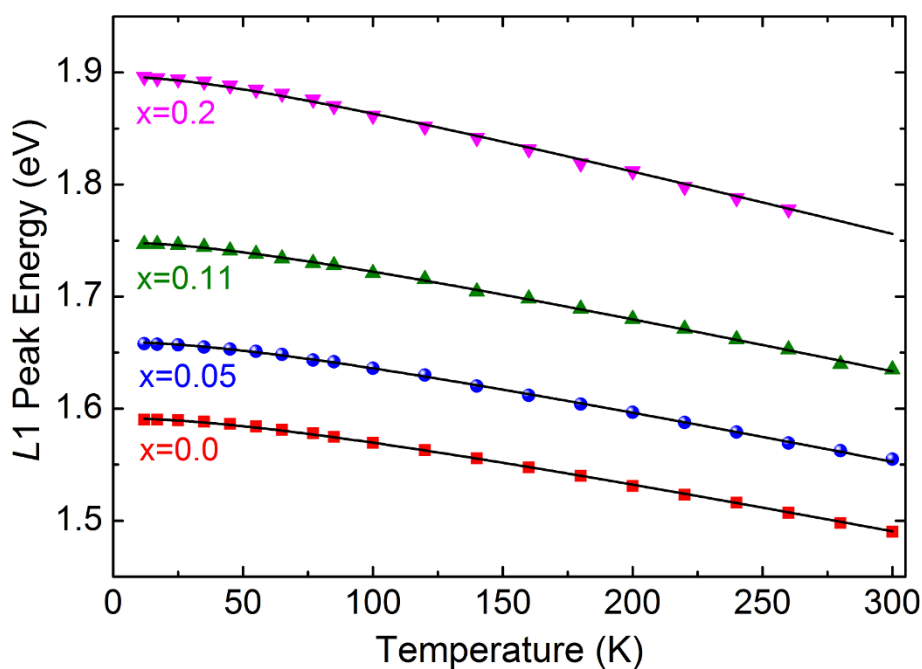


Figure 2 Temperature dependence of the neutral acceptor-bound exciton peak L1 for a series of Mn concentrations. The solid lines are the fits according to the Varshni relation (Equation 1).

Table 1 Values of the parameters obtained by fitting the energy gap vs temperature to Equation 1

Mn <i>x</i>	E_0 (eV)	α (10^{-4} eV/k)	β (K)	$-dE_g/dT$ ($77 \leq T \leq 300$) (10^{-4} eV/k)
0.0	1.592	0.00046	110	3.94
0.05	1.660	0.00048	104	4.07
0.11	1.748	0.0005	91	4.36
0.2	1.896	0.00059	78	5.25

the observed increase in the parameter α with increasing x in $Zn_{1-x}Mn_xSe$ [16]. The decrease of β seen in Table 1 is another feature characteristic of Mn-based DMS alloys [16]. It is well known that in a semiconductor, when the temperature is much below the Debye temperature, a T^2 dependence of the energy gap is observed, a behavior which led Varshni to propose a relation between the parameter β in Equation 1 and Debye temperature θ_D [13]. In Mn-based DMSs the Debye temperature does not change with increasing Mn concentrations [17]. We therefore believe that there is an additional factor which increases the gap. Alexander et al. [18] analyzed this phenomenon as being due to the shift of the conduction band energy resulting from the exchange interaction between the magnetic ions and conduction electrons. We are thus inclined to conclude that the decrease in β with x is connected with a smooth shift of the conduction-band energy [19].

Figure 3 shows the temperature dependence of the full width at half maximum [FWHM] of the L1 emission line

with Mn concentration x . With increasing Mn mole fraction x , the FWHM of the L1 emission line varies from approximately 3.02 meV for $x = 0.0$ to approximately 9.49 meV for $x = 0.2$. The FWHM of the L1 emission line also increases with increasing temperature, which can be accounted for by increasing the exciton-phonon interaction at higher temperatures. The temperature dependence of the emission linewidth caused by exciton-phonon interactions has the form [20]

$$\Gamma(T) = \Gamma_{inh} + \gamma_{LA}T + \frac{\Gamma_{LO}}{\exp(\hbar\omega_{LO}/k_B T) - 1} + \Gamma_i \exp(E_i/k_B T), \quad (2)$$

where Γ_{inh} is the inhomogeneous broadening term, γ_{LA} is a coefficient of exciton-acoustic phonon interaction, Γ_{LO} is the exciton-LO phonon coupling constant, $\hbar\omega_{LO}$ is the LO phonon energy, Γ_i is a proportionality factor which accounts for the concentration of impurity centers, and E_i is the binding energy of impurity-bound excitons averaged over all possible locations of the impurities. The solid lines in Figure 3 are drawn by fitting Equation 2 to the experiment data. In the case of CdTe, the fitted values are $\Gamma_{inh} = 1.15$ meV, $\Gamma_{LO} = 25.6$ meV, $\hbar\omega_{LO} = 20.9$ meV, and $\gamma_{LA} = 4.9 \times 10^{-6}$ meV. It is noted here that the contribution of the impurity scattering process to the linewidth broadening can be neglected. The value for $\hbar\omega_{LO}$ is in good agreement with the LO phonon energy of 21.3 meV in CdTe [6]. Listed in Table 2 are the obtained values of Γ_{inh} , Γ_{LO} , $\hbar\omega_{LO}$, and γ_{LA} for the $Cd_{1-x}Mn_xTe$ crystals. We noted that the effect of γ_{LA} is smaller than that of any other

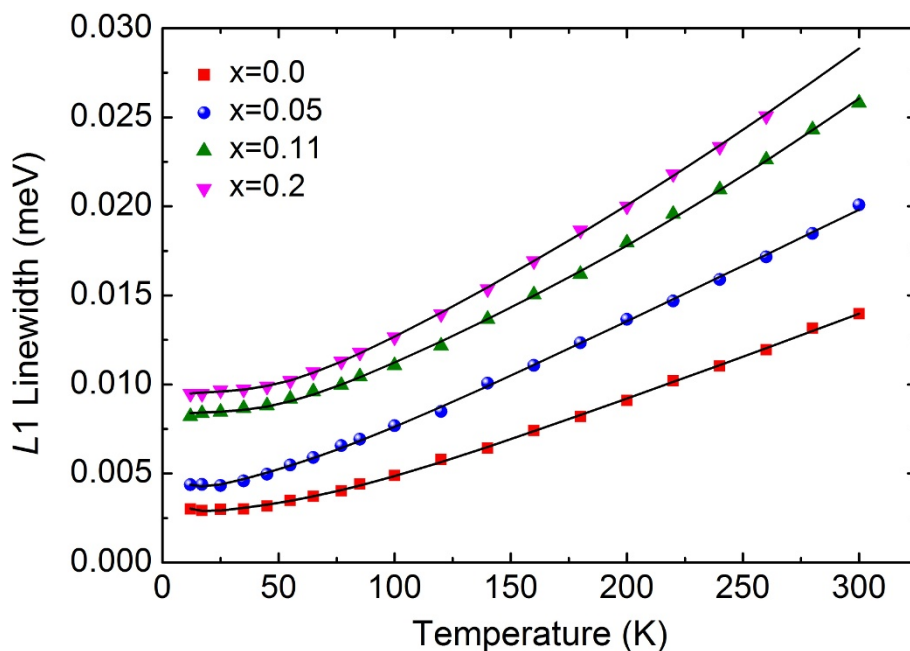


Figure 3 Temperature dependence of the FWHM of L1 emission lines for a series of Mn concentrations.

Table 2 Values of Γ_{inh} , Γ_{LO} , $\hbar\omega_{LO}$, and γ_{LA} and the behaviors of activation energies

Mn x	Γ_{inh} (meV)	Γ_{LO} (meV)	$\hbar\omega_{LO}$ (meV)	γ_{LA} (10^{-6} meV)	E_1 (meV)	E_2 (meV)
0.0	1.15	25.6	20.98	4.9	5.9	17.18
0.05	1.65	26.14	21.0	1.0	5.38	16.67
0.11	2.0	27.06	21.01	1.8	4.89	15.81
0.2	3.53	28.44	21.03	2.3	4.22	14.39

Parameters on Γ_{inh} , Γ_{LO} , $\hbar\omega_{LO}$, and γ_{LA} as a function of Mn concentration x were obtained by fitting Equation 2 to the data shown in Figure 3. Also listed are the obtained values of E_1 and E_2 , obtained by fitting Equation 3 to the data shown in Figure 4.

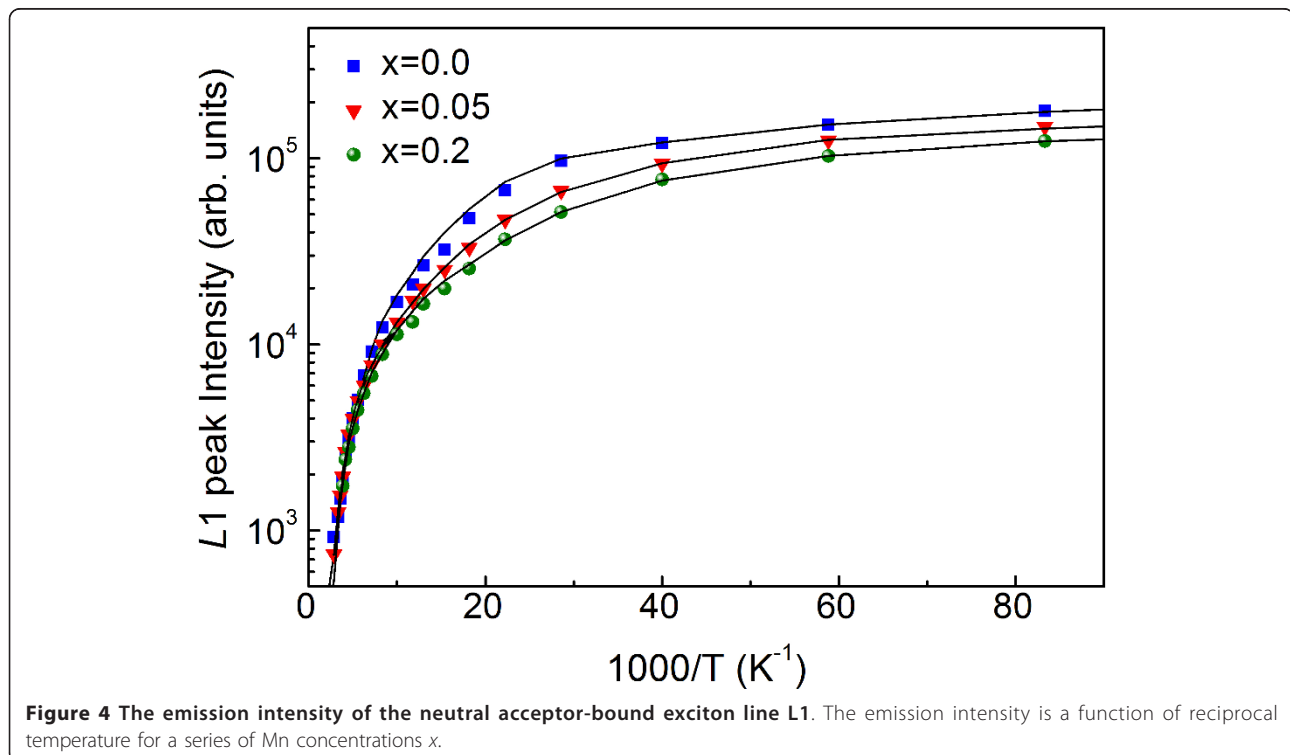
broadening term for each composition x , indicating that the effect of exciton-acoustic phonon interaction on the linewidth is negligible. It is noted that Γ_{inh} and Γ_{LO} increase with increasing x , while $\hbar\omega_{LO}$ is nearly constant. It is well known that Γ_{LO} should increase with the polarity of the material and that the inhomogeneous broadening in Γ_{inh} may be accounted for implicitly and partly by the presence of various site symmetries of the Mn^{2+} ion in the lattice, the existence of stacking faults [21], and the presence of impurity complexes involving lattice vacancies [22].

Figure 4 shows the L1 luminescence intensity of CMT crystals as a function of reciprocal temperature in the range from 12 K to 300 K. It is recognized that a host of different processes contribute to reduction of the PL intensity as temperature increases. As observed in other semiconductors [23], the temperature dependence of the

luminescence intensity shows a two-step quenching process and can be expressed in the form

$$I(T) = \frac{I_0}{1 + C_1 \exp(-E_1/kT) + C_2 \exp(-E_2/kT)}, \quad (3)$$

where E_1 and E_2 are the high- and low-temperature activation energies, respectively. For CdTe, the values of the parameters obtained from the fit to Equation 3 are $E_1 = 5.9$ meV and $E_2 = 14.3$ meV. These values are in fairly good agreement with the reported exciton binding energies for the L1 line [24]. Listed in Table 2 are the behaviors of activation energies as a function of Mn mole fraction x . The activation energy is seen to decrease with increasing Mn concentration, similar to the results reported by Su et al. [25]. This behavior has been interpreted in terms of the four-center model



suggested by Fonger [26] and observed in many ternary alloys [27,28].

Conclusion

The PL characteristics of the diluted magnetic semiconductor alloy CMT crystals were systematically studied as a function of temperature and Mn concentrations. Bulk crystals were grown by the vertical Bridgman method for Mn concentrations from $x = 0.0$ to 0.2 . Our studies involved near-band-edge excitonic PL emission of neutral acceptor-bound excitons with emphasis on the dependence of the PL spectrum on temperature and alloy composition. With increasing x , the Varshni parameter α increased while β decreased. From the temperature dependence of the FWHM of the L1 emission line, the broadening factors were determined by fitting Equation 2 to the data. From the temperature dependence of L1 we were able to determine the activation energies for thermal quenching of the corresponding bound excitons. Our results showed that the values of activation energies decrease with increasing Mn concentration x .

Acknowledgements

This work was supported by the Nuclear R&D program (2010-0026181) and the Priority Research Centers Program (2009-0093818) through the National Research Foundation of Korea (NRF), funded by the Ministry of Education, Science, and Technology.

Author details

¹Basic Science Research Institute, University of Ulsan, Ulsan, 680-749, South Korea ²Department of Physics, University of Ulsan, Ulsan, 680-749, South Korea ³Department of Semiconductor Applications, Ulsan College, Ulsan, 680-749, South Korea

Authors' contributions

YH carried out the CdMnTe crystal growth and wrote this manuscript. YU participated in the design of this research and performed the data analysis. HP participated in the measurement of photoluminescence and analysis. All authors read and approved the final manuscript.

Competing interests

The authors declare that they have no competing interests.

Received: 9 September 2011 Accepted: 5 January 2012

Published: 5 January 2012

References

1. Furdyna JK: Diluted magnetic semiconductors. *J Appl Phys* 1988, **64**:R29.
2. Kavokin KV, Merkulov IA, Yakovlev DR, Ossau W, Landwehr G: Exciton localization in semimagnetic semiconductors probed by magnetic polarons. *Phys Rev B* 1999, **60**:16499-16505.
3. Mycielski A, Kowalczyk L, Galazka RR, Sobolewski R, Wang D, Burger A, Sowinska M, Groza M, Siffert P, Szadkowski A, Witkowska B, Kaliszek W: Applications of II-VI semimagnetic semiconductors. *J Alloys Compd* 2006, **423**:163-168.
4. Kim KH, Camarda GS, Bolotnikov AE, James RB, Hong J, Kim S: Improved carrier-transport properties of passivated CdMnTe crystals. *J Appl Phys* 2009, **105**:093705.
5. Pavesi L, Guzzi M: Photoluminescence of $\text{Al}_x\text{Ga}_{1-x}\text{As}$ alloys. *J Appl Phys* 1994, **75**:4779-4842.
6. Halliday DP, Potter MDG, Mullins JT, Brinkman AW: Photoluminescence study of a bulk vapour grown CdTe crystal. *J Crystal Growth* 2000, **220**:30-38.

7. Palosz W, Graszka K, Boyd PR, Cui Y, Wright G, Roy UN, Burger A: Photoluminescence of CdTe crystals grown by physical-vapor transport. *J Electron Mater* 2003, **32**:747-751.
8. Taguchi T, Onodera C: Shallow acceptor bound-excitons in CdTe Epitaxial layers on (100) GaAs. *Mat Sci Forum* 1990, **65**:235-240.
9. Francou JM, Saminadayar K, Pautrat JL: Shallow donors in CdTe. *Phys Rev B* 1990, **41**:12035-12046.
10. Oda O: Compound semiconductor bulk materials and characterizations. World scientific Publishing. Co. Pte. Ltd; 2007, 422-424.
11. Becla P, Kaiser D, Giles NC, Lansari Y, Schetzina JF: Electrical and optical properties of P- and As-doped $\text{Cd}_{1-x}\text{Mn}_x\text{Te}$. *J Appl Phys* 1987, **62**:1352-1362.
12. Lautenschlager P, Logothetidis S, Viña L, Cardona M: Ellipsometric studies of the dielectric function of $\text{Cd}_{1-x}\text{Mn}_x\text{Te}$ alloys. *Phys Rev B* 1985, **32**:3811-3818.
13. Varshni YP: Temperature dependence of the energy gap in semiconductors. *Physica* 1967, **34**:149-154.
14. Heine V, Van Vechten JA: Effect of electron-hole pairs on phonon frequencies in Si related to temperature dependence of band gaps. *Phys Rev B* 1976, **13**:1622-1626.
15. Bottka N, Stankiewicz J, Girit W: Electroreflectance studies in $\text{Cd}_{1-x}\text{Mn}_x\text{Te}$ solid solutions. *J Appl Phys* 1981, **52**:4189-4193.
16. Bylsma RB, Becker WM, Kossut J, Debska U: Dependence of energy gap on x and T in $\text{Zn}_{1-x}\text{Mn}_x\text{Se}$: the role of exchange interaction. *Phys Rev B* 1986, **33**:8207-8215.
17. Galazka RR, Nagata S, Keesom PH: Paramagnetic-spin-glass-antiferromagnetic phase transitions in $\text{Cd}_{1-x}\text{Mn}_x\text{Te}$ from specific heat and magnetic susceptibility measurements. *Phys Rev B* 1980, **22**:3344-3355.
18. Alexander S, Helman JS, Balberg I: Critical behavior of the electrical resistivity in magnetic systems. *Phys Rev B* 1976, **13**:304-315.
19. Diouri J, Lascaray JP, El Amrani M: Effect of the magnetic order on the optical-absorption edge in $\text{Cd}_{1-x}\text{Mn}_x\text{Te}$. *Phys Rev B* 1985, **31**:7995-7999.
20. Rudin S, Reinecke TL, Segall B: Temperature-dependent exciton linewidths in semiconductors. *Phys Rev B* 1990, **42**:11218-11231.
21. Lanver U, Lehmann G: Luminescence spectra of Mn(II) in different symmetries. *J Lumin* 1978, **17**:225-235.
22. Sibley WA, Koumvakalis N: Perturbed Mn^{2+} transitions in irradiated $\text{RbMgF}_3\text{:Mn}$. *Phys Rev B* 1976, **14**:35-40.
23. Bimberg D, Sondergeld M, Grobe E: Thermal dissociation of excitons bounds to neutral acceptors in high-purity GaAs. *Phys Rev B* 1971, **4**:3451-3455.
24. Cohen E, Street RA, Muranevich A: Bound excitons and resonant Raman scattering in $\text{Cd}_x\text{Zn}_{1-x}\text{Te}$ ($0.9 \leq x \leq 1$). *Phys Rev B* 1983, **28**:7115-7124.
25. Su JS, Wang JC, Chen YF, Shen JL, Chou WC: Dielectric studies of $\text{Zn}_{1-x}\text{Mn}_x\text{Se}$ epilayers. *J Appl Phys* 1999, **86**:1630-1633.
26. Fonger WH: Nearest-neighbor splitting of the luminescence levels of $\text{ZnS}_x\text{Se}_{1-x}$. *Phys Rev* 1965, **137**:A1038-A1048.
27. Block D, Cox RT: Optically detected magnetic resonance of donor-center pairs in $\text{ZnS}_x\text{Se}_{1-x}$ ($x = 0.995$). *J Lumin* 1981, **24-25**:167-171.
28. Zunger A: Composition-dependence of deep impurity levels in alloys. *Phys Rev Lett* 1985, **54**:849.

doi:10.1186/1556-276X-7-36

Cite this article as: Hwang et al.: Photoluminescence characteristics of $\text{Cd}_{1-x}\text{Mn}_x\text{Te}$ single crystals grown by the vertical Bridgman method. *Nanoscale Research Letters* 2012 **7**:36.